Archival Report

Biological Psychiatry

Social Synchronization of Conditioned Fear in Mice Requires Ventral Hippocampus Input to the Amygdala

Wataru Ito, Alexander J. Palmer, and Alexei Morozov

ABSTRACT

BACKGROUND: Social organisms synchronize behaviors as an evolutionary-conserved means of thriving. Synchronization under threat, in particular, benefits survival and occurs across species, including humans, but the underlying mechanisms remain unknown because of the scarcity of relevant animal models. Here, we developed a rodent paradigm in which mice synchronized a classically conditioned fear response and identified an underlying neuronal circuit.

METHODS: Male and female mice were trained individually using auditory fear conditioning and then tested 24 hours later as dyads while allowing unrestricted social interaction during exposure to the conditioned stimulus under visible or infrared illumination to eliminate visual cues. The synchronization of the immobility or freezing bouts was quantified by calculating the effect size Cohen's *d* for the difference between the actual freezing time overlap and the overlap by chance. The inactivation of the dorsomedial prefrontal cortex, dorsal hippocampus, or ventral hippocampus was achieved by local infusions of muscimol. The chemogenetic disconnection of the hippocampus-amygdala pathway was performed by expressing hM4D(Gi) in the ventral hippocampal neurons and infusing clozapine *N*-oxide in the amygdala.

RESULTS: Mice synchronized cued but not contextual fear. It was higher in males than in females and attenuated in the absence of visible light. Inactivation of the ventral but not dorsal hippocampus or dorsomedial prefrontal cortex abolished fear synchronization. Finally, the disconnection of the hippocampus-amygdala pathway diminished fear synchronization.

CONCLUSIONS: Mice synchronize expression of conditioned fear relying on the ventral hippocampus-amygdala pathway, suggesting that the hippocampus transmits social information to the amygdala to synchronize threat response.

https://doi.org/10.1016/j.biopsych.2022.07.016

From invertebrates to humans, social organisms coordinate various activities, including defense from predators, foraging, raising progeny, and migration (1–5). One simple form of coordination is aligning of movement (1,6). In humans, it is called nonverbal interpersonal synchrony and is an indicator of social normality. It correlates with prosocial behaviors; it is increased by oxytocin and decreased in schizophrenia, borderline personality disorder, and autism (7–13).

While many species coordinate body movement (1), only a few publications report such coordination in rodents. For example, rats shuttle together to obtain reward in an operant task (14) and aggregate in response to predator smell or bright light (15–17). Mice aggregate in the presence of a spider robot, and being inside the aggregation attenuates the threat-induced gamma oscillations in the amygdala (18). Prairie voles follow the leader animal to generate a uniform response to an owl attack (19–21). These examples of coordinated threat responses suggest that rodents can be used to study basic mechanisms of emotional synchronization. Although the mouse is a gregarious species with robust social modulation of threat responses (22–27), no study has established a quantitative paradigm for social synchronization of threat response in mice. Here, we provide such a paradigm based on the classical Pavlovian conditioning and identify a neuronal circuit essential for synchronization of classically conditioned fear response.

METHODS AND MATERIALS

All experiments were performed according to a Virginia Tech Institutional Animal Care and Use Committee–approved protocol.

Animals

Breeding trios of one C57BL/6N male and two 129SvEv females produced 129SvEv/C57BL/6N F1 hybrid male and female mice, weaned at postnatal day (p) 21 and housed as 4 littermates per cage with the same sex as described (23). Animals underwent tests at p75 to p90. Seven to 10 days

ISSN: 0006-3223

before testing, mice were split 2 per clean cage with a quarter of the Nestlet material (Ancare) from the originating cage.

Fear Conditioning

Mice in each dyad were trained independently in 2 separate conditioning chambers (Med Associates) as described (28) and then tested together as dyads in a single chamber. For cued fear training, each animal spent the first 2 minutes in the chamber without stimuli and then received 4 pairings of the conditioned stimulus (CS) and unconditioned stimulus (US) given at variable intervals (60–180 seconds). The CS was a 30-second, 8 kHz, 80-dB tone, and the US was a 0.5 mA, 0.5-second electrical shock co-terminated with CS. Mice returned to the home cage 30 seconds after the last CS-US pairing. Cued fear was tested once 1 day later or twice 1 day and 3 days later in the DREADD (designer receptors exclusively activated by designer drugs) experiments and in the muscimol inactivation of the ventral hippocampus (vHPC). First, the animals spent 1 minute in a new context without CS and 2 minutes with CS. For contextual fear training, each animal spent 2.5 minutes in the chamber without stimuli and then received three 0.8 mA, 2-second footshocks separated by 1 minute and returned to the home cage 30 seconds after the last shock. Contextual fear was tested 1 day later by placing the dyads in the training chamber for 3 minutes. Videos were recorded at 4 frames per second, exported as AVI files with MJPEG compression using the FreezeFrame system (Actimetrics), and then converted to the mp4 format using a Python script.

Quantification of Freezing, Freezing Overlap, Freezing Synchrony, and Leader-Follower Relationship

Annotators, unaware of the treatment of the animals, manually identified and recorded the first and last video frames of each freezing bout using a Python script. A freezing bout was defined as a lack of movement, except for respiration, for at least 4 consecutive video frames. From the annotation, another Python script generated the freezing duration for each animal, freezing overlap for each dyad (duration of simultaneous freezing), and graphic representation of their temporal dynamics. We defined freezing synchrony as the standardized difference (Cohen's *d* effect size) between the observed and chance freezing overlaps. The chance overlaps were obtained by performing 1000 random circular permutations of the freezing timelines and computing the freezing overlap for each. The synchrony was obtained by subtracting the mean of chance overlaps from the observed overlap and dividing it by the standard deviation of chance overlaps.

To evaluate the leader-follower relationship within each dyad, we calculated the leadership bias and percent maximum leadership. First, dyad members were assigned arbitrarily as #1 and #2 or, when one of the two animals was cannulated, as #1 for the cannulated and #2 for the noncannulated member. Then, we counted the matched transitions, in which one animal (follower) followed another (initiator), and summated the counts as the leadership bias using +1 when animal #1 was the initiator and −1 when animal #2 was the initiator (Figure S14). In the case of perfect leadership, where one member always takes the leadership, the absolute value of the leadership bias equals the total number of the matched transitions (theoretical maximum). To standardize the leadership measure across dyads, we expressed leadership bias as a percentage of the theoretical maximum (percent maximum leadership) at the end of the test session. The signed percent maximum leadership identifies the leader animal (positive for animal #1 and negative for animal #2).

Surgeries and Intracranial Infusions

Viral Injections. Pseudotype 5 viral vectors pAAV-hSyn-hM4D(Gi) (Addgene), pAAV-hSyn-EGFP (Addgene), or pAAV-hSyn-Chronos-GFP (UNC Vector Core) at a titer of 10^{12} viral particles per milliliter were injected bilaterally in 2 locations, 0.2 μL per site, targeting the intermediate HPC (from bregma: −3.4 mm posterior, ±3.4 mm lateral; from the brain surface: −1.65 mm ventral) and the vHPC (from bregma: −3.4 mm posterior, ±3.8 mm lateral; from the brain surface: −2.6 mm ventral) following the surgical procedure described in (29).

Cannulation. Ten to 14 days before fear conditioning, the mice received implantation bilaterally with guide cannulas, made in the laboratory from hypodermic tubes or purchased from P1 Technologies to target the dorsomedial prefrontal cortex (dmPFC) (from bregma: 1.5 mm anterior, ±0.5 mm lateral; from the brain surface: −0.8 mm ventral), vHPC (from bregma: −3.3 mm posterior, ±3.3 mm lateral; from the brain surface −2.8 mm ventral), or basolateral amygdala (BLA) (from bregma: −1.8 mm posterior, ±3.2 mm lateral; from the brain surface −3.5 mm ventral). Dummy cannulas were placed in the guide cannulas to prevent clogging.

Intracranial Infusion. During the 7 days before testing, animals were handled for 2 to 3 minutes daily, including for removal and reattachment of dummy cannulas. One day before fear conditioning training, mice were habituated to infusion using vehicle: (in mM) 150 NaCl, 10 D-glucose, 10 HEPES, 2.5 KCl, 1 $MgCl_2$, pH 7.35 (30) in the home cage in the presence of the partner. The infusion cannula extended 1 mm over the guide cannula. The infusion volume was always 150 nL per site, and the infusion rate was 75 nL/min. Muscimol (1.17 mM) or vehicle was infused 1 hour before fear testing. In DREADD experiments, the infusate was clozapine *N*-oxide (CNO) (3 μM) or vehicle, infused 45 to 50 minutes before testing. In all experiments, except in Figure 3D, E, both mice in the same dyad received identical infusions.

Position Verification for Cannulas and Viral Transduction. After the final test, each animal, anesthetized with 2.5% Avertin (prepared by mixing 10 g of 2,2,2-tribromoethyl alcohol [T4,840-2; Sigma-Aldrich] with 10 mL of tert-amyl alcohol [24,048–6; Sigma-Aldrich], diluted 1:40 by phosphate-buffered saline and filter sterilization), received an intracranial infusion of Chicago Sky Blue (C8679; Sigma-Aldrich) (0.2%), followed by transcardial perfusion with 4% paraformaldehyde. Fluorescent and visible light microscopy identified the sites of viral transduction and cannulation.

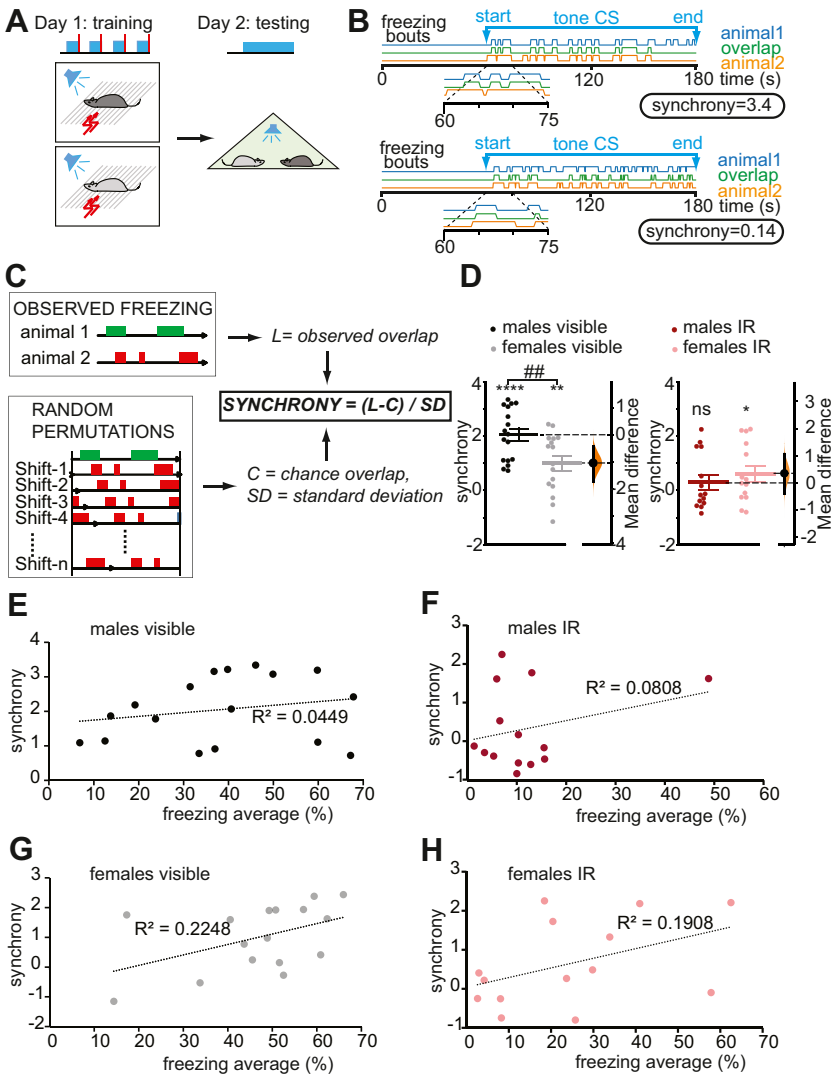

Figure 1. Synchronization of auditory fear differs between sexes and relies on vision more strongly in males than in females. **(A)** Scheme for testing fear synchrony. Fear conditioning training on day 1 and testing on day 2. Blue rectangles and red vertical bars represent CS and US, respectively. **(B)** Examples of freezing timelines in dyads with high (upper, synchrony = 3.4) and low (lower, synchrony = 0.14) freezing synchrony. CS onsets at 60 seconds are zoomed in. Freezing bouts of animals 1 and 2 are shown in blue and orange, respectively, and freezing overlaps in green. **(C)** Computing freezing synchrony. The observed freezing overlap L is taken from the freezing timelines. The timelines are then randomly permutated 1000 times, giving 1000 permutated overlaps, from which the mean chance overlap C and the standard deviation are calculated. SYNCHRONY = (L − C)/SD. **(D)** Summary diagrams for synchrony in male and female dyads tested under visible or IR light. Independent dyads were tested under visible and IR light. Horizontal bars indicate mean ± SEM. The visible synchrony panel (left) includes the effect size as a bootstrap 95% CI (vertical line) and the resampled distribution of the mean difference (orange) computed by DABEST (32) (https://www.estimationstats.com/#/). The effect size is aligned with the mean of the female test groups. Under visible light, synchrony was significant in both sexes (one-sample t test: males: $p < .0001$, $n = 17$; females: $p = .002$, $n = 16$) and higher in males (two-sample t test: $p = .007$). Under IR light, synchrony was not significant in males (Wilcoxon signed-rank test: $n = 14$) but significant in females (one-sample t test: $p < .05$, $n = 14$). One-sample t test: $^{*}p < .05$, $^{**}p < .01$, $^{****}p < .0001$; two-sample t test: $^{\#\#}p < .01$. **(E–H)** Scatter plots of synchrony vs. freezing in males under visible light **(E)**, males under IR light **(F)**, females under visible light **(G)**, and females under IR light **(H)**. Freezing (%) is the average of 2 mice in each dyad. No significant correlation was found. C, chance overlap; CS, conditioned stimulus; IR, infrared; L, observed overlap; ns, not significant; US, unconditioned stimulus.

Whole-Cell Recording

Slice preparation and whole-cell recording from amygdala neurons were done as described in (31). Briefly, the internal solution of the recording pipette was 120 K-gluconate (in mM), 5 NaCl, 1 $MgCl_2$, 10 HEPES, 0.2 EGTA, 2 ATP-Mg, and 0.1 GTP-Na. Four hundred seventy nanometer 1-ms light pulses from an LED lamp (Thorlabs) through ×40 objective lens (Olympus) stimulated the hippocampal axons expressing Chronos at 0.3 to 2.5 mW every 30 seconds. Stimulus intensity was adjusted to obtain excitatory postsynaptic currents at about 80% of the maximum.

Data Analysis

Statistical analyses were performed using GraphPad Prism 5 (GraphPad Software) and Python scripts using SciPy statistical functions (scipy.stats), and R. Normality was tested using the Shapiro-Wilk test (Table S3). Datasets with normal distribution were compared using the one-sample t test or the paired t test as indicated. The datasets with non-normal distribution were compared using the Mann-Whitney test, the Wilcoxon matched-pairs test, and the Wilcoxon signed-rank test. All the tests were two-sided. The two-tailed p value was calculated for the Spearman correlation analysis. The effects were deemed significant with $p < .05$. The effect size as a bootstrap 95% CI was computed and plotted using the data analysis with bootstrap-coupled estimation in Python 1 (32). For each comparison, 5000 reshuffles of each group were performed.

Data and Code Availability

All primary data, including video files, are available from the authors upon reasonable request. In addition, codes for data analysis and statistics are provided with example data as part of the replication package. These are available at https://github.com/wataruito/codes_in_Emotional_sync_Ito_et_al.

RESULTS

To study synchronization of fear response, we trained mice individually and then tested them in dyads of cage mates on the following day. During training, repeated auditory CS were paired with electrical footshocks as the US. During testing, mice were allowed unrestricted social interaction while exposed to CS in a different context (Figure 1A). To quantify the synchrony of freezing within each dyad, we calculated the Cohen's *d* effect size for the simultaneous freezing above chance. As shown in Figure 1C, the difference between the observed freezing overlap (L) and the mean of permutation-generated freezing overlaps (C: chance overlap) was divided by the standard deviation of the chance overlaps (Figure 1B, C).

Both sexes synchronized freezing but males synchronized more than females (Figure 1D, left). In males, synchrony did not correlate with the following freezing measures: percent freezing average, percent freezing of the high freezer, percent freezing of the low freezer, and the difference of percent freezing between high and low freezers (Figure 1E; Figure S1), the mean duration, or the number of freezing bouts (Figure S3 and Table S2). In female mice, synchrony did not correlate with any freezing measure except for a weak correlation with percent freezing of the low freezer (R^2 = 0.3, p = .03) (Figure 1G; Figure S1) and the mean duration of freezing bouts (Figure S3 and Table S2).

Visual, auditory, olfactory, and somatosensory social cues can convey information about the partner's state. Testing dyads under infrared (IR) illumination aimed to examine the role of vision. Most males failed to synchronize, whereas most females synchronized (p = .048) (Figure 1D, right), and there was a significant sex × lighting interaction ($F_{1,57}$ = 7.0, p = .015). The freezing under the IR light was lower in both sexes (males: $p < .0001$, females: p = .005) (Figure 1E–H), consistent with earlier findings (33). Nevertheless, synchrony did not correlate with the freezing measures (Figure 1F, H; Figure S1).

To examine synchronization of contextual fear, we trained a separate cohort of males by exposing them to electrical footshocks and tested them in the training context 24 hours later. Unlike cued freezing, the mice did not synchronize bouts of contextual freezing (Figure S12). Notably, in all the above cohorts, freezing strongly correlated between partners regardless of the level of fear synchrony (Figure S2 and Table S1).

In search of the brain regions involved in synchronization, we focused on 3 areas, the dmPFC, dorsal HPC (dHPC), and vHPC. These regions all encode social information (34–37), contribute to social memory (37), and modulate fear expression (22,38–41). Therefore, each structure can contribute to integrating social and emotional information required for synchronized freezing. To this end, each structure was inactivated by bilateral muscimol infusion (Figure 2A, B, E, H) in both animals of each dyad 1 hour before testing. These experiments were performed on males because males synchronized more strongly than females. The vHPC inactivation diminished synchrony without affecting freezing (Figure 2I, J) and duration or number of freezing bouts (Figure S5). Inactivation of the dHPC or dmPFC did not attenuate synchrony but decreased freezing (Figure 2C, F), consistent with the described effects of such inactivation on fear expression (38,42–44). Synchrony did not correlate with freezing measures of the dyad (Figure 2D, G, J; Figure S4) in any experiment.

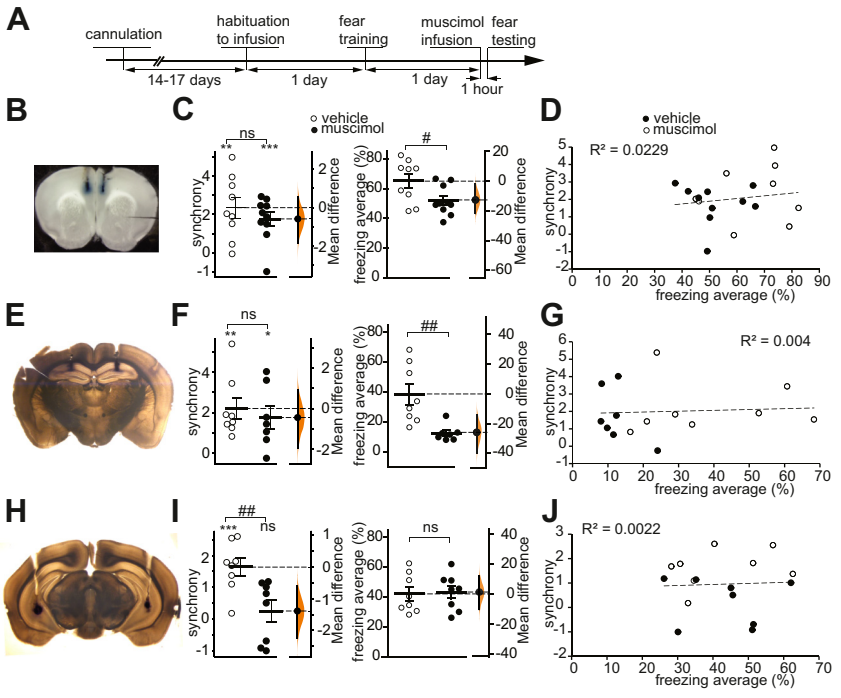

Figure 2. Fear synchrony requires the vHPC. **(A)** Experimental timeline. Independent dyads were infused with vehicle or muscimol. **(B, E, H)** Examples of dye injections in the muscimol inactivation sites in the dmPFC **(B)**, dHPC **(E)**, and vHPC **(H)**. **(C, F, I)** Summary diagrams for synchrony (left) and percent freezing average (right) in dyads with both mice injected in the dmPFC **(C)** (n = 9/10 with vehicle/muscimol), dHPC **(F)** (n = 8/7), and vHPC **(I)** (n = 8/8). For synchrony, comparisons to 0 were made by the one-sample t test in panel **(C)** and Wilcoxon signed-rank test in panels **(F)** and **(I)**. For synchrony and freezing average, comparisons between groups were made by the two-sample t test in panel **(C)** and Mann-Whitney test in panels **(F)** and **(I)**. $^{*}p < .05$, $^{\#}p < .05$, $^{**}p < .01$, $^{\#\#}p < .01$, $^{***}p < .001$. Horizontal bars indicate mean ± SEM. The resampled distribution of the mean difference (orange) and the 95% CI (vertical line) are shown on the right. The effect size is aligned with the mean of the test group (muscimol). **(D, G, J)** Scatter plots of synchrony vs. freezing for the dmPFC **(D)**, dHPC **(G)**, and vHPC **(J)** inactivation experiments. Freezing (%) is the average of 2 mice in each dyad. No significant correlation was found. dHPC, dorsal hippocampus; dmPFC, dorsomedial prefrontal cortex; ns, not significant; vHPC, ventral hippocampus.

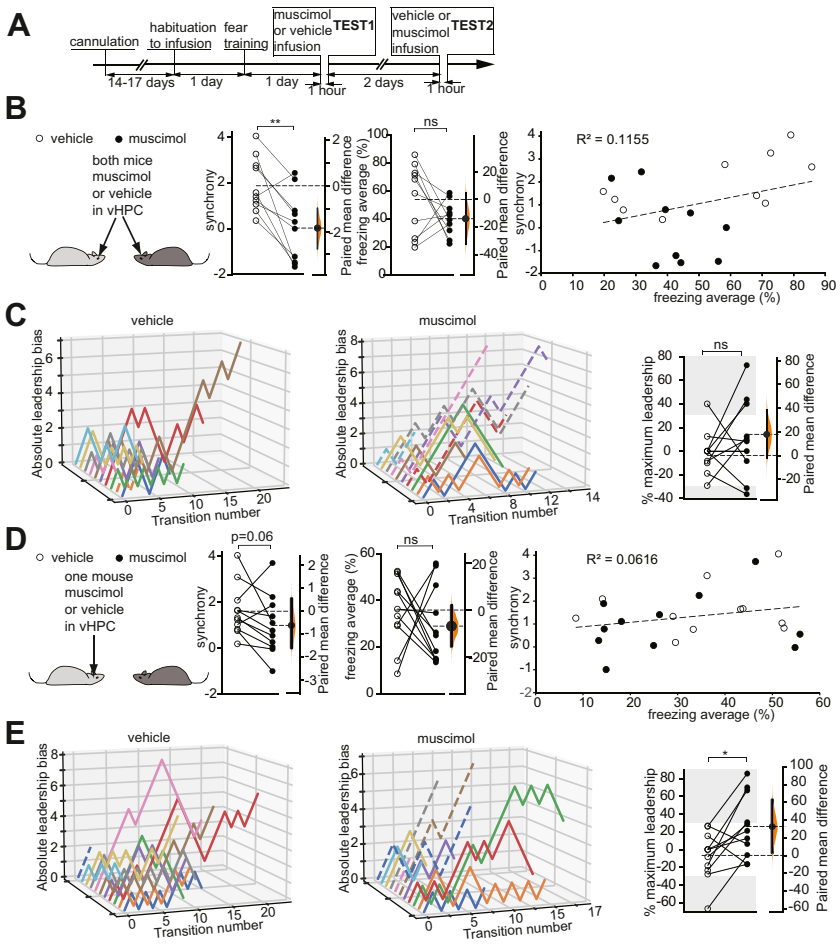

Figure 3. vHPC is required for synchrony and suppresses leadership. **(A)** Experimental scheme of behavioral testing with muscimol suppression. **(B, D)** Left: Schematics of muscimol injections. Right: Summary diagrams of synchrony (left), percent freezing averages of both dyad members (middle), and freezing synchrony scatter plot (right). No significant correlation was found. Open and black circles represent dyads infused with vehicle and muscimol, respectively ($n = 10$) **(B)**, 11 dyads **(C)**. **(C, E)** Left and middle: Trajectories of the absolute leadership bias along the matched transitions. Dashed lines represent dyads with the percent maximum leadership above 30%. Right: Percent maximum leadership after infusion of vehicle and muscimol. The gray shades represent the >30% and <−30% cutoffs. Connected data points represent the same dyad. Positive and negative percent maximum leadership indicates that animal 1 or 2 exhibited stronger leadership, respectively. In panel **(C)**, 1 and 2 were assigned arbitrarily. In panel **(E)**, 1 was assigned to the animal receiving infusions. Wilcoxon matched-pairs test: $^*p < .05$. The resampled mean difference distribution (orange) and the 95% CI (vertical line) are shown. The effect size is aligned with the mean of the test group (muscimol). ns, not significant; vHPC, ventral hippocampus.

To confirm the role of the vHPC in synchrony and examine how the vHPC determines the leader of the freezing transitions, we repeated the muscimol infusion experiments but within the dyad comparisons to absorb the effects of variability among individual dyads. After training, all dyads were tested twice: 24 hours (test 1) and 72 hours (test 2) later. We ran 2 independent cohorts: both dyad members received muscimol or vehicle infusion in the vHPC (cohort 1), or only 1 member received the infusions (cohort 2). The order of infusion was counterbalanced between muscimol and vehicle (Figure 3A). The repeated testing per se caused fear extinction but had no effects on synchrony (Figure S8). Muscimol significantly decreased synchrony in cohort 1 (Figure 3B), reconfirming that the vHPC is needed for synchrony, but not in cohort 2 (Figure 3D), indicating that synchrony remains when one of the animals has a functional vHPC. Muscimol had no effect on percent freezing or duration and the number of freezing bouts (Figure S7), and synchrony did not correlate with freezing measures (Figure 3B, D; Figure S6).

Next, we calculated the leadership bias as the difference between the numbers of freezing transitions led by the members of the dyad, and the percent maximum leadership as the normalized leadership bias. In the case of perfect leadership, when animal 1 or 2 leads all freezing transitions, the leadership bias is + (total transition number) or − (total transition number), and the percent maximum leadership is +100% or −100%, respectively (explained in Methods and Materials; Figure S14).

Among the 2 cohorts, in 73.8% of test sessions (31 of 42), the percent maximum leadership was below 30%, and there was little or no progressive increase in the absolute leadership bias along with the transition number (Figure 3C, E, left and middle, solid lines), indicating the lack of strong leaders. However, muscimol infusion increased the number of dyads with higher percent maximum leadership (above 30%) from 1 to 5 in cohort 1 and from 1 to 4 in cohort 2 (Figure 3C, E, left and middle, broken lines). When only 1 mouse received muscimol (cohort 2), that mouse took more leadership, as shown by significantly increased percent maximum leadership (Figure 3E, right). Furthermore, the increase was observed regardless of the leadership status (leader or follower) when injected with vehicle. In contrast, when both mice received muscimol infusion (cohort 1), the percent maximum leadership did not change (Figure 3C, right).

The input from the vHPC to the amygdala is necessary for context-dependent control of cued fear (45,46). The

hippocampal-amygdala axons originate primarily from the CA1 and subicular neurons in the temporal/caudal half of the Ammon's horn, which includes the ventral and intermediate HPC (here collectively referred to as vHPC) (47,48). To test whether these axons are necessary for the social synchronization of freezing, we chemogenetically suppressed their terminals in the amygdala. Whole-cell recording confirmed the effectiveness of such suppression, using amygdala slices from mice coinjected with AAV-hSyn-hM4Di-mCherry and AAV-hSynChronos-GFP in the HPC. One micromolar CNO in the bath suppressed excitatory postsynaptic currents evoked in BLA neurons by blue light pulses by 90.4 ± 3.8% (Figure 4A).

For behavioral testing, we injected the mice with AAV-hSyn-hM4Di-mCherry in the vHPC (Figure 4C), 25 to 30 days later implanted cannulas for CNO infusion in the BLA and allowed the mice to recover for 14 to 17 days.

All dyads were tested twice, at 24 hours (test 1) and 72 hours (test 2) after training. Forty minutes before each test, the mice received CNO or vehicle infusion in the BLA in counterbalanced order (Figure 4B). The infusions were counterbalanced because repeated testing per se caused fear extinction in some cohorts, although it did not affect synchrony (Figure S11). In male mice, CNO decreased synchrony but had no effect on percent freezing (Figure 4D upper) or the duration or number of freezing bouts (Figure S10). Synchrony also did not correlate with freezing measures (Figure S9). In female mice, CNO decreased synchrony and freezing (Figure 4E, upper). It also decreased the duration of freezing bouts but not the number of bouts (Figure S10). Despite the strong effect of CNO on both synchrony and freezing in female mice, synchrony only correlated with percent freezing in the low freezers, and the correlation was weak (R^2 = 0.18, p = .03) (Figure S9). To control for the nonspecific effects of CNO, separate groups of mice underwent the same procedures, except that they received AAV-hSyn-GFP (6 male dyads) or AAV-hSyn-Chronos-GFP (4 male and all female dyads). CNO had no effect on synchrony or freezing, and there was no correlation between synchrony and freezing measures, even in

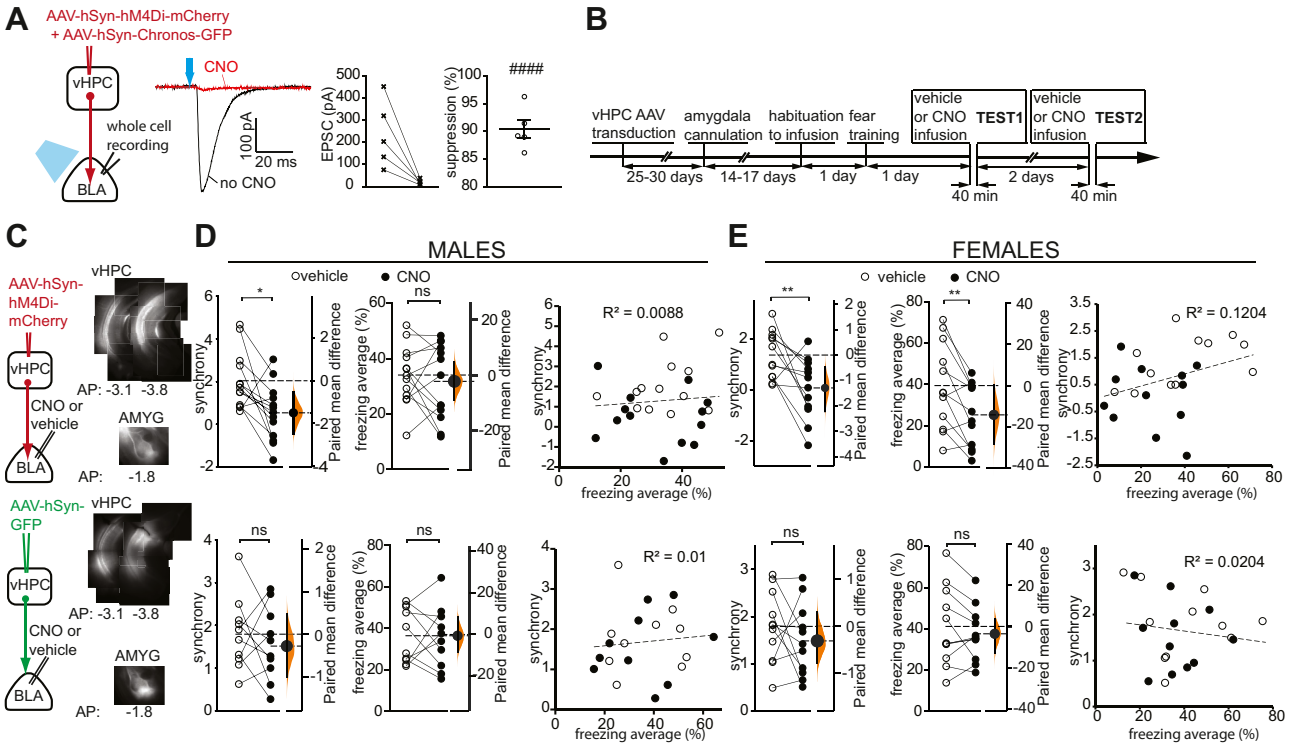

Figure 4. Fear synchrony requires the vHPC input to the amygdala. **(A)** DREADD suppression of the vHPC terminals in the BLA ex vivo. Left: Schematics of viral injection, ex vivo stimulation, and whole-cell recording. Middle: Example of EPSC evoked in a BLA neuron by blue light stimulation of the vHPC terminals in the absence of CNO (black), and after 10 minutes of perfusion with 1-μM CNO (red), shown as averages of 5 consecutive sweeps. Right: Summary of EPSC changes (no CNO vs. CNO), recorded from 5 BLA neurons, and percent suppression by 1-μM CNO. Wilcoxon signed-rank test: ####$p < .0001$. Horizontal bars indicate mean ± SEM. **(B)** Experimental scheme of behavioral testing with DREADD suppression. **(C)** Left: Schematics of viral injection and cannula placement. Right: Fluorescent images of the vHPC and the amygdala slices from mice injected with AAV-hSyn-hM4Di-mCherry (upper row) and AAV-hSyn-GFP (lower row) in the ventral/intermediate hippocampus. **(D, E)** Summary diagrams (males in panel **D**, females in panel **E**) of synchrony (left), percent freezing average (middle), and freezing synchrony scatter plot (right) in the dyads expressing hM4Di-mCherry (upper row, DREADD disconnection, n = 13 [male], 12 [female]) or GFP or Chronos-GFP (lower row, CNO/virus controls, n = 10 [male], 11 [female]), both mice in the dyad infused with vehicle (open circle) or 3-μM CNO (black filled circle) in the amygdala. No significant correlation was found in panels **(D)** and **(E)** in the right most column. The connected data points represent the same dyads. Freezing (%) is the average of 2 mice in each dyad. Wilcoxon matched-pairs test: *$p < .05$, **$p < .01$. The resampled mean difference distribution (orange) and the 95% CI (vertical line) are shown. The effect size is aligned with the mean of the test group (CNO). AMYG, amygdala; AP, anterior-posterior; BLA, basolateral amygdala; CNO, clozapine *N*-oxide; DREADD, designer receptors exclusively activated by designer drugs; EPSC, excitatory postsynaptic current; ns, not significant; vHPC, ventral hippocampus.

the female group (Figure 4D, E, lower; Figure S9). In all cohorts in DREADD disconnection and muscimol inactivation experiments, synchrony and freezing did not change significantly between the first and second halves of the session (Figure S13).

DISCUSSION

The main goal of this work was to establish a mouse paradigm and a quantitative measure for social synchronization of an affective behavior. The key findings are that freely interacting mice synchronize freezing response to an auditory CS and that the vHPC to the amygdala pathway is required for this synchronization.

Most studies on behavioral synchrony focus on rhythmic movements. They define synchrony as the degree of congruence between the behavioral cycles of 2 subjects (49) and quantify it by coherence and cross-correlation (7,8,10,50).

Such metrics are not applicable in this study because of limited sampling: testing of conditioned fear is limited to a few minutes and not repeatable multiple times. The resulting small number of freezing bouts is insufficient for evaluating rhythmicity or periodicity. Therefore, we defined synchrony more broadly as simultaneous affect (51) and operationally as simultaneous behavior (49). We quantified synchrony based on the duration of simultaneous freezing or freezing overlap. Because there is, however, always some overlap occurring by chance, which increases with higher freezing, we calculated freezing synchrony as the difference between the observed freezing overlap and the freezing overlap by chance, normalized to the standard deviation of the chance overlap. This metric factors out the chance overlap and allows for comparison among dyads with different levels of freezing. In fact, throughout this study, synchrony in most cohorts did not correlate with freezing measures, which included the percent freezing average of dyad members, percent freezing of the high and low freezer, percent freezing difference between dyad members, and duration or number of freezing bouts. It suggests that most animals respond to social cues and coordinate behavior independently from the level of fear. As an exception, in some but not all female cohorts, synchrony correlated with freezing of the low freezer and with duration of freezing bouts, but the correlation was weak. Nevertheless, they suggest differences in how males and females integrate social and emotional information.

While both sexes synchronized freezing, males synchronized it more than females, suggesting sex differences within the circuits involved in synchronization. One mouse study reported lower sociability in females (52), which could explain the lower synchrony. However, other studies did not detect sex differences in the sociability of mice (53,54), suggesting that sociability and synchrony require separate circuits. The lack of synchrony in most male dyads under IR light suggests that males rely primarily on vision, whereas the ability of most females to synchronize suggests that they can use other sensory modalities. On the other hand, the freezing level under IR was lower for both sexes. It may result from fear reduction and (or) a switch from passive (freezing) to active (escape) threat response (55). Therefore, the sex differences in synchrony under IR may arise at the fear expression level, not only from the different reliance on vision.

Fear synchrony did not require the dmPFC, similar to dmPFC independence of social motivation in mice (56,57), although the dmPFC was found necessary for social motivation in a rat study (58). Meanwhile, dmPFC-dependent social cognition drives empathy-like behavior and hierarchy formation (59). Perhaps, social motivation and synchrony are evolutionarily older, making them less dependent on the PFC. However, our study does not rule out that the dmPFC modulates fear synchrony, just as it modulates social motivation (59).

Inactivation of the vHPC or its terminals inside the amygdala disrupted fear synchrony. Given the reports of the hippocampal involvement in the attention process (60) and, in particular, the role of the vHPC in the attention tasks in rodents (61), the impaired synchrony can arise from the loss of attention. Furthermore, the recently discovered social neurons in the vHPC (62) can participate in social attention, potentially encode conspecific information and route it to the amygdala.

Notably, the vHPC inactivation or disconnection from the amygdala did not change the overall freezing level but diminished synchronization. This suggests that the role of the social neurons is to adjust the temporal pattern of the amygdala activity but not its level. Two types of hippocampal commands, which initiate and terminate freezing, could provide such temporal adjustments. The reported parallel pathways, excitatory hippocampal-amygdala input to the basal and central nuclei (46,47), and GABAergic (gamma-aminobutyric acidergic) input to the basal amygdala (63,64) might transmit the opposing commands.

Our analysis of the leader-follower relationship revealed that most dyads did not have fixed leaders driving the transitions in and out of freezing; instead, the leadership is flexible, and dyad members followed one another. However, when the vHPC was inactivated in only 1 mouse in a dyad, the treated mouse increased the leadership, suggesting that the vHPC is required for the ability to follow the partner.

The contextual freezing showed no synchronization. One hypothesis is that the contextual fear circuitry lacks the mechanism for the accurate timing of events. Indeed, bed nucleus of the stria terminalis, which is required for contextual fear expression, mediates fear responses when the timing of an aversive event is uncertain (65–67); therefore, it is unlikely to respond precisely to the partner's behavioral transitions. Another hypothesis is based on 2 facts: testing context fear activates the dHPC (68–70), and the dHPC strongly projects to the vHPC through the longitudinal pathway via CA2 (71–73). The activated dHPC may interfere with the vHPC via the CA2 route and prevent it from processing social cues.

Overall, this study adds one example to the list of synchronized behaviors in several species (74), the conditioned freezing in mice, and opens up studies of synchronized behaviors in mice.

ACKNOWLEDGMENTS AND DISCLOSURES

This work was supported by the National Institutes of Health (Grant Nos. MH120290 and MH118604 [to AM]).

The authors report no biomedical financial interests or potential conflicts of interest.

ARTICLE INFORMATION

From the Fralin Biomedical Research Institute at Virginia Tech Carilion Center for Neurobiology Research (WI, AJP, AM) and Carilion Clinic

Department of Psychiatry and Behavioral Medicine (AM), Roanoke, Virginia.

Address correspondence to Alexei Morozov, Ph.D., at alexeim@vtc.vt.edu, or Wataru Ito, Ph.D., at wataru.ito@gmail.com.

Received Dec 14, 2021; revised Jun 17, 2022; accepted Jul 11, 2022.

Supplementary material cited in this article is available online at https://doi.org/10.1016/j.biopsych.2022.07.016.

REFERENCES

1. Herbert-Read JE (2016): Understanding how animal groups achieve coordinated movement. J Exp Biol 219:2971–2983.
2. Bazazi S, Pfennig KS, Handegard NO, Couzin ID (2012): Vortex formation and foraging in polyphenic spadefoot toad tadpoles. Behav Ecol Sociobiol 66:879–889.
3. Codling EA, Pitchford JW, Simpson SD (2007): Group navigation and the "many-wrongs principle" in models of animal movement. Ecology 88:1864–1870.
4. Seeley TD, Buhrman SC (1999): Group decision making in swarms of honey bees. Behav Ecol Sociobiol 45:19–31.
5. Grünbaum D (1998): Schooling as a strategy for taxis in a noisy environment. Evol Ecol 12:503–522.
6. Duranton C, Gaunet F (2016): Behavioural synchronization from an ethological perspective: Overview of its adaptive value. Adapt Behav 24:181–191.
7. Kupper Z, Ramseyer F, Hoffmann H, Tschacher W (2015): Nonverbal synchrony in social interactions of patients with schizophrenia indicates socio-communicative deficits. PLoS One 10:e0145882.
8. Ramseyer F, Ebert A, Roser P, Edel MA, Tschacher W, Brüne M (2020): Exploring nonverbal synchrony in borderline personality disorder: A double-blind placebo-controlled study using oxytocin. Br J Clin Psychol 59:186–207.
9. Curioni A, Minio-Paluello I, Sacheli LM, Candidi M, Aglioti SM (2017): Autistic traits affect interpersonal motor coordination by modulating strategic use of role-based behavior. Mol Autism 8:23.
10. Georgescu AL, Koeroglu S, Hamilton AFC, Vogeley K, Falter-Wagner CM, Tschacher W (2020): Reduced nonverbal interpersonal synchrony in autism spectrum disorder independent of partner diagnosis: A motion energy study. Mol Autism 11:11.
11. McNaughton KA, Redcay E (2020): Interpersonal synchrony in autism. Curr Psychiatry Rep 22:12.
12. Rennung M, Göritz AS (2016): Prosocial consequences of interpersonal synchrony: A meta-analysis. Z Psychol 224:168–189.
13. Wiltermuth SS, Heath C (2009): Synchrony and cooperation. Psychol Sci 20:1–5.
14. Swanson HH, Schuster R (1987): Cooperative social coordination and aggression in male laboratory rats – Effects of housing and testosterone. Horm Behav 21:310–330.
15. Bowen MT, Keats K, Kendig MD, Cakic V, Callaghan PD, McGregor IS (2012): Aggregation in quads but not pairs of rats exposed to cat odor or bright light. Behav Process 90:331–336.
16. Bowen MT, McGregor IS (2014): Oxytocin and vasopressin modulate the social response to threat: A preclinical study. Int J Neuropsychopharmacol 17:1621–1633.
17. Bowen MT, Kevin RC, May M, Staples LG, Hunt GE, McGregor IS (2013): Defensive aggregation (huddling) in Rattus norvegicus toward predator odor: Individual differences, social buffering effects and neural correlates. PLoS One 8:e68483.
18. Kim J, Kim C, Han HB, Cho CJ, Yeom W, Lee SQ, Choi JH (2020): A bird's-eye view of brain activity in socially interacting mice through mobile edge computing (MEC). Sci Adv 6:eabb9841.
19. Izhar R, Eilam D (2010): Together they stand: A life-threatening event reduces individual behavioral variability in groups of voles. Behav Brain Res 208:282–285.
20. Eilam D, Zadicario P, Genossar T, Mort J (2012): The anxious vole: The impact of group and gender on collective behavior under life-threat. Behav Ecol Sociobiol 66:959–968.
21. Rabi C, Zadicario P, Mazon Y, Wagner N, Eilam D (2017): The response of social and non-social rodents to owl attack. Behav Ecol Sociobiol 71.
22. Jeon D, Kim S, Chetana M, Jo D, Ruley HE, Lin SY, *et al.* (2010): Observational fear learning involves affective pain system and Cav1.2 Ca2+ channels in ACC. Nat Neurosci 13:482–488.
23. Ito W, Erisir A, Morozov A (2015): Observation of distressed conspecific as a model of emotional trauma generates silent synapses in the prefrontal-amygdala pathway and enhances fear learning, but ketamine abolishes those effects. Neuropsychopharmacology 40:2536–2545.
24. Morozov A, Ito W (2019): Social modulation of fear: Facilitation vs buffering. Genes Brain Behav 18:e12491.
25. Allsop SA, Wichmann R, Mills F, Burgos-Robles A, Chang CJ, Felix-Ortiz AC, *et al.* (2018): Corticoamygdala transfer of socially derived information gates observational learning. Cell 173:1329–1342.e18.
26. Chen Q, Panksepp JB, Lahvis GP (2009): Empathy is moderated by genetic background in mice. PLoS One 4:e4387.
27. Langford DJ, Crager SE, Shehzad Z, Smith SB, Sotocinal SG, Levenstadt JS, *et al.* (2006): Social modulation of pain as evidence for empathy in mice. Science 312:1967–1970.
28. Pan BX, Vautier F, Ito W, Bolshakov VY, Morozov A (2008): Enhanced cortico-amygdala efficacy and suppressed fear in absence of Rap1. J Neurosci 28:2089–2098.
29. Ito W, Morozov A (2019): Prefrontal-amygdala plasticity enabled by observational fear. Neuropsychopharmacology 44:1778–1787.
30. Stachniak TJ, Ghosh A, Sternson SM (2014): Chemogenetic synaptic silencing of neural circuits localizes a hypothalamus→midbrain pathway for feeding behavior. Neuron 82:797–808.
31. Morozov A, Sukato D, Ito W (2011): Selective suppression of plasticity in amygdala inputs from temporal association cortex by the external capsule. J Neurosci 31:339–345.
32. Ho J, Tumkaya T, Aryal S, Choi H, Claridge-Chang A (2019): Moving beyond P values: Data analysis with estimation graphics. Nat Methods 16:565–566.
33. Warthen DM, Wiltgen BJ, Provencio I (2011): Light enhances learned fear. Proc Natl Acad Sci U S A 108:13788–13793.
34. Li Z, Lu YF, Li CL, Wang Y, Sun W, He T, *et al.* (2014): Social interaction with a cagemate in pain facilitates subsequent spinal nociception via activation of the medial prefrontal cortex in rats. Pain 155:1253–1261.
35. Hitti FL, Siegelbaum SA (2014): The hippocampal CA2 region is essential for social memory. Nature 508:88–92.
36. Okuyama T, Kitamura T, Roy DS, Itohara S, Tonegawa S (2016): Ventral CA1 neurons store social memory. Science 353:1536–1541.
37. Phillips ML, Robinson HA, Pozzo-Miller L (2019): Ventral hippocampal projections to the medial prefrontal cortex regulate social memory. eLife 8.
38. Sierra-Mercado D, Padilla-Coreano N, Quirk GJ (2011): Dissociable roles of prelimbic and infralimbic cortices, ventral hippocampus, and basolateral amygdala in the expression and extinction of conditioned fear. Neuropsychopharmacology 36:529–538.
39. Izquierdo I, Furini CR, Myskiw JC (2016): Fear memory. Physiol Rev 96:695–750.
40. Giustino TF, Maren S (2015): The role of the medial prefrontal cortex in the conditioning and extinction of fear. Front Behav Neurosci 9:298.
41. Ortiz S, Latsko MS, Fouty JL, Dutta S, Adkins JM, Jasnow AM (2019): Anterior cingulate cortex and ventral hippocampal inputs to the basolateral amygdala selectively control generalized fear. J Neurosci 39:6526–6539.
42. Laurent V, Westbrook RF (2009): Inactivation of the infralimbic but not the prelimbic cortex impairs consolidation and retrieval of fear extinction. Learn Mem 16:520–529.
43. Holt W, Maren S (1999): Muscimol inactivation of the dorsal hippocampus impairs contextual retrieval of fear memory. J Neurosci 19:9054–9062.
44. Quinn JJ, Wied HM, Ma QD, Tinsley MR, Fanselow MS (2008): Dorsal hippocampus involvement in delay fear conditioning depends upon

the strength of the tone-footshock association. Hippocampus 18:640–654.
45. Orsini CA, Kim JH, Knapska E, Maren S (2011): Hippocampal and prefrontal projections to the basal amygdala mediate contextual regulation of fear after extinction. J Neurosci 31:17269–17277.
46. Xu C, Krabbe S, Gründemann J, Botta P, Fadok JP, Osakada F, *et al.* (2016): Distinct hippocampal pathways mediate dissociable roles of context in memory retrieval. Cell 167:961–972.e916.
47. Kishi T, Tsumori T, Yokota S, Yasui Y (2006): Topographical projection from the hippocampal formation to the amygdala: A combined anterograde and retrograde tracing study in the rat. J Comp Neurol 496:349–368.
48. Fanselow MS, Dong HW (2010): Are the dorsal and ventral hippocampus functionally distinct structures? Neuron 65:7–19.
49. Bernieri FJ, Reznick JS, Rosenthal R (1988): Synchrony, pseudosynchrony, and dyssynchrony: Measuring the entrainment process in mother infant interactions. J Pers Soc Psychol 54:243–253.
50. Jiang Y, Platt ML (2018): Oxytocin and vasopressin flatten dominance hierarchy and enhance behavioral synchrony in part via anterior cingulate cortex. Sci Rep 8:8201.
51. Siegman AW, Reynolds M (1982): Interviewer-interviewee nonverbal communications: An interactional approach. In: Davis M, editor. Interaction Rhythms: Periodicity in Communicative Behavior. New York: Human Sciences Press, 249–277.
52. Defensor EB, Pearson BL, Pobbe RL, Bolivar VJ, Blanchard DC, Blanchard RJ (2011): A novel social proximity test suggests patterns of social avoidance and gaze aversion-like behavior in BTBR T+ tf/J mice. Behav Brain Res 217:302–308.
53. Silverman JL, Tolu SS, Barkan CL, Crawley JN (2010): Repetitive self-grooming behavior in the BTBR mouse model of autism is blocked by the mGluR5 antagonist MPEP. Neuropsychopharmacology 35:976–989.
54. Yang M, Clarke AM, Crawley JN (2009): Postnatal lesion evidence against a primary role for the corpus callosum in mouse sociability. Eur J Neurosci 29:1663–1677.
55. Mongeau R, Miller GA, Chiang E, Anderson DJ (2003): Neural correlates of competing fear behaviors evoked by an innately aversive stimulus. J Neurosci 23:3855–3868.
56. Avale ME, Chabout J, Pons S, Serreau P, De Chaumont F, Olivo-Marin JC, *et al.* (2011): Prefrontal nicotinic receptors control novel social interaction between mice. FASEB J 25:2145–2155.
57. Yizhar O, Fenno LE, Prigge M, Schneider F, Davidson TJ, O'Shea DJ, *et al.* (2011): Neocortical excitation/inhibition balance in information processing and social dysfunction. Nature 477:171–178.
58. Rudebeck PH, Walton ME, Millette BH, Shirley E, Rushworth MF, Bannerman DM (2007): Distinct contributions of frontal areas to emotion and social behaviour in the rat. Eur J Neurosci 26:2315–2326.
59. Bicks LK, Koike H, Akbarian S, Morishita H (2015): Prefrontal cortex and social cognition in mouse and man. Front Psychol 6:1805.
60. Aly M, Turk-Browne NB (2017): How hippocampal memory shapes, and is shaped by, attention. In: Hannula D, Duff M, editors. The Hippocampus From Cells to Systems. Cham, Germany: Springer.
61. Li X, Chen W, Pan K, Li H, Pang P, Guo Y, *et al.* (2018): Serotonin receptor 2c-expressing cells in the ventral CA1 control attention via innervation of the Edinger–Westphal nucleus. Nat Neurosci 21:1239–1250.
62. Rao RP, von Heimendahl M, Bahr V, Brecht M (2019): Neuronal responses to conspecifics in the ventral CA1. Cell Rep 27:3460–3472.e3.
63. Lübkemann R, Eberhardt J, Röhl FW, Janitzky K, Nullmeier S, Stork O, *et al.* (2015): Identification and characterization of GABAergic projection neurons from ventral hippocampus to amygdala. Brain Sci 5:299–317.
64. McDonald AJ, Mott DD (2017): Functional neuroanatomy of amygdalohippocampal interconnections and their role in learning and memory. J Neurosci Res 95:797–820.
65. Goode TD, Maren S (2017): Role of the bed nucleus of the stria terminalis in aversive learning and memory. Learn Mem 24:480–491.
66. Goode TD, Ressler RL, Acca GM, Miles OW, Maren S (2019): Bed nucleus of the stria terminalis regulates fear to unpredictable threat signals. eLife 8:e46525.
67. Haufler D, Nagy FZ, Pare D (2013): Neuronal correlates of fear conditioning in the bed nucleus of the stria terminalis. Learn Mem 20:633–641.
68. Maviel T, Durkin TP, Menzaghi F, Bontempi B (2004): Sites of neocortical reorganization critical for remote spatial memory. Science 305:96–99.
69. Squire LR, Genzel L, Wixted JT, Morris RG (2015): Memory consolidation. Cold Spring Harb Perspect Biol 7:a021766.
70. Preston AR, Eichenbaum H (2013): Interplay of hippocampus and prefrontal cortex in memory. Curr Biol 23:R764–R773.
71. Kohara K, Pignatelli M, Rivest AJ, Jung HY, Kitamura T, Suh J, *et al.* (2014): Cell type-specific genetic and optogenetic tools reveal hippocampal CA2 circuits. Nat Neurosci 17:269–279.
72. Tamamaki N, Abe K, Nojyo Y (1988): Three-dimensional analysis of the whole axonal arbors originating from single CA2 pyramidal neurons in the rat hippocampus with the aid of a computer graphic technique. Brain Res 452:255–272.
73. Meira T, Leroy F, Buss EW, Oliva A, Park J, Siegelbaum SA (2018): A hippocampal circuit linking dorsal CA2 to ventral CA1 critical for social memory dynamics. Nat Commun 9:4163.
74. Duranton C, Bedossa T, Gaunet F (2017): Interspecific behavioural synchronization: Dogs exhibit locomotor synchrony with humans. Sci Rep 7:12384.